Supplementary Information (SI) for Nanoscale Horizons.
This journal is © The Royal Society of Chemistry 2026

Supporting Information

An Acoustic Sensing Fabric based on PVDF-HFP Nanofiber Core-Shell Yarns for Respiratory Acoustic Signal Monitoring

Jinjin Song,[a] Haifan Tang,[a] Junyun Zhang,[a] Jiaxue Yu,[a] Dailin Yuan,[a] Yanqiu Zhang,[a] Jinyang Wang,[a] Di Pan,[a] Weixu Tian,[a] Jingye Jin,*[a] Jian Fang*[b] and Chenhong Lang*[a]

* Corresponding author.

[a] *State Key Laboratory of Bio-based Fiber Materials, College of Textile Science and Engineering (International Institute of Silk), Zhejiang Sci-Tech University, Hangzhou 310018, China. E-mail addresses: chlang@zstu.edu.cn; jin_jingye@zstu.edu.cn.*

[b] *National Engineering Laboratory for Modern Silk, College of Textile and Clothing Engineering, Soochow University, Suzhou 215123, China. E-mail addresses: jian.fang@suda.edu.cn*

Materials	Device type	Working mechanism	Device size (cm^2)	Output voltage (V)	Frequency response range (Hz)	Maximum sensitivity ($mV\ Pa^{-1}$)	Refs
PVDF	Fiber-based	Piezo-Tribo	2.5 × 2.5	70.9	10-500	10050.6	1
PVDF/BN	Fiber-based	Piezo-Tribo	3 × 4	174.2	230-5000	15500	2
PVDF-TrFE /MXene	Fiber-based	Piezo-Tribo	4 × 4	42.3	50-1000	37000	3
PVDF/MOF	Fiber-based	Piezo	4 × 4	6	20-330	950	4
PAN, PA6	Fiber-based	Tribo	19.6	0.612	20-5000	715	5
PVDF/rGO	Yarn-based	Piezo	1 cm (length)	0.0075	50-1000	6.22	6
PVDF-TrFE /$BaTiO_3$	Fabric-based	Piezo	8 × 8	0.002	80-1000	19.6	7
PMMA, PTFE	Fabric-based	Optical	24 × 24	/	70-320	17.48	8
PVDF-HFP	Fabric-based	Piezo-Tribo	2 × 2	38.3	170-1010	2500	this work

Table. S1 Comparison of the performance of all-fiber acoustic sensors.

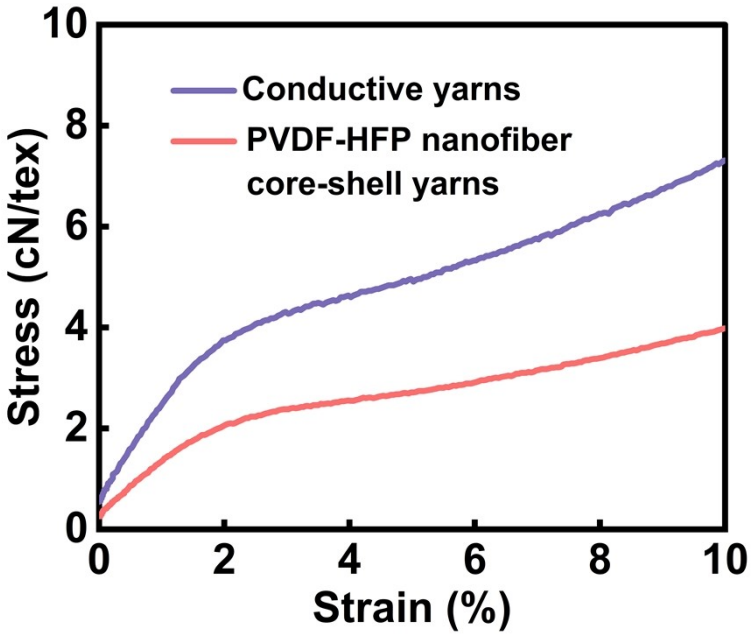

Fig. S1: Stress-strain curves of conductive yarns and PVDF-HFP core-shell yarns.

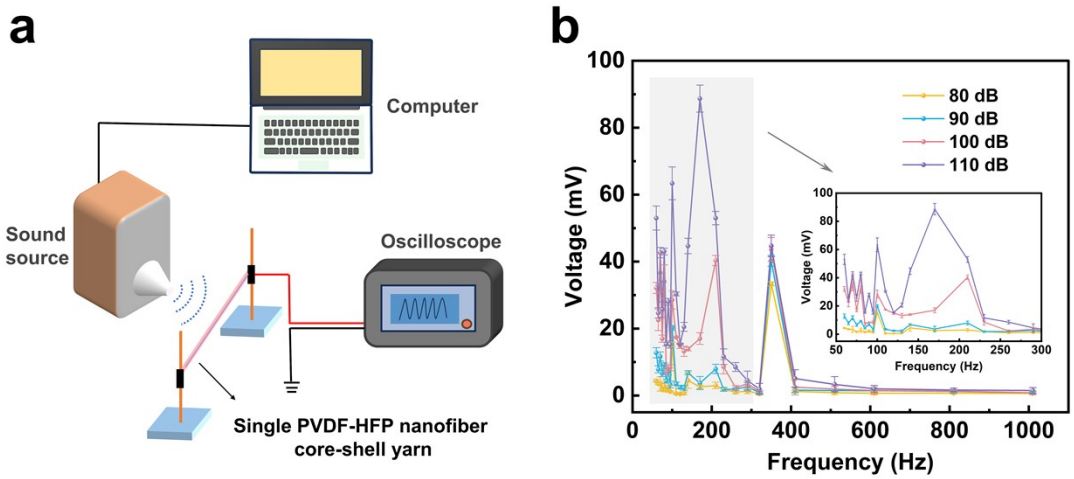

Fig. S2: (a) Schematic illustration of the setup for single PVDF-HFP nanofiber yarn, (b) Dependence of voltage outputs on sound frequency at four different sound pressure levels for single PVDF-HFP nanofiber core-shell yarn.

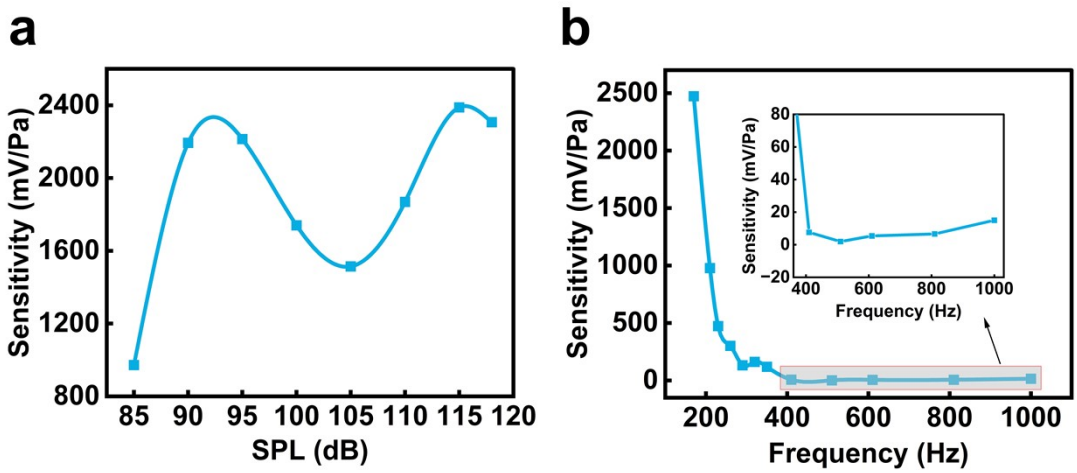

Fig. S3: The sensitivity profile of ASF (a) across the 85-118 dB sound pressure range (frequency, 170 Hz) and (b) across the 170-1000 Hz sound frequency range (sound pressure level, 94 dB).

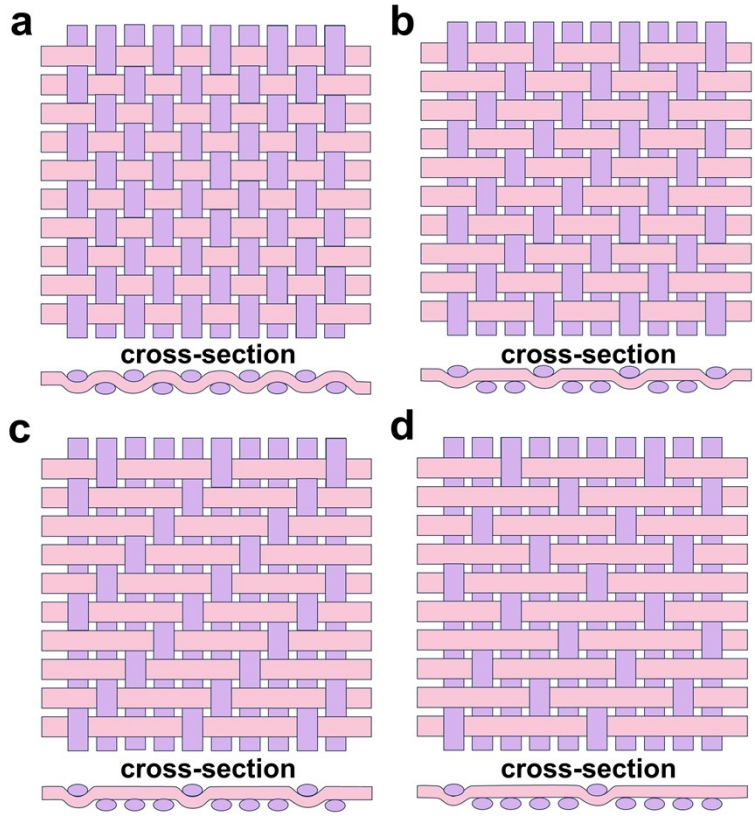

Fig. S4: The schematic diagrams of the fabric structure (a) plain weave, (b) 1/2 twill weave, (c) 1/3 twill weave, and (d) sateen weave.

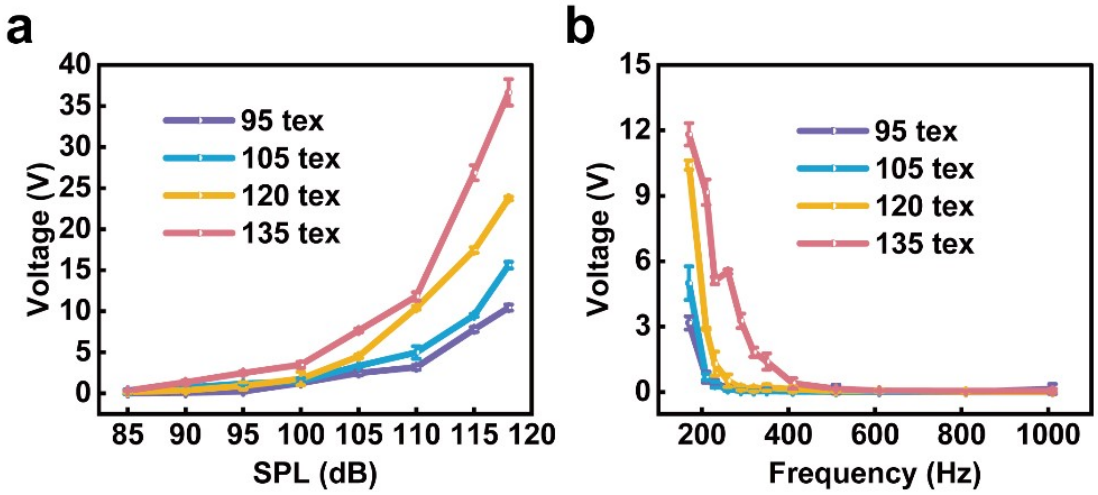

Fig. S5: Influence of weft fineness on (a) sound pressure response properties (frequency, 170 Hz) and (b) frequency response properties (SPL, 110 dB) of ASF.

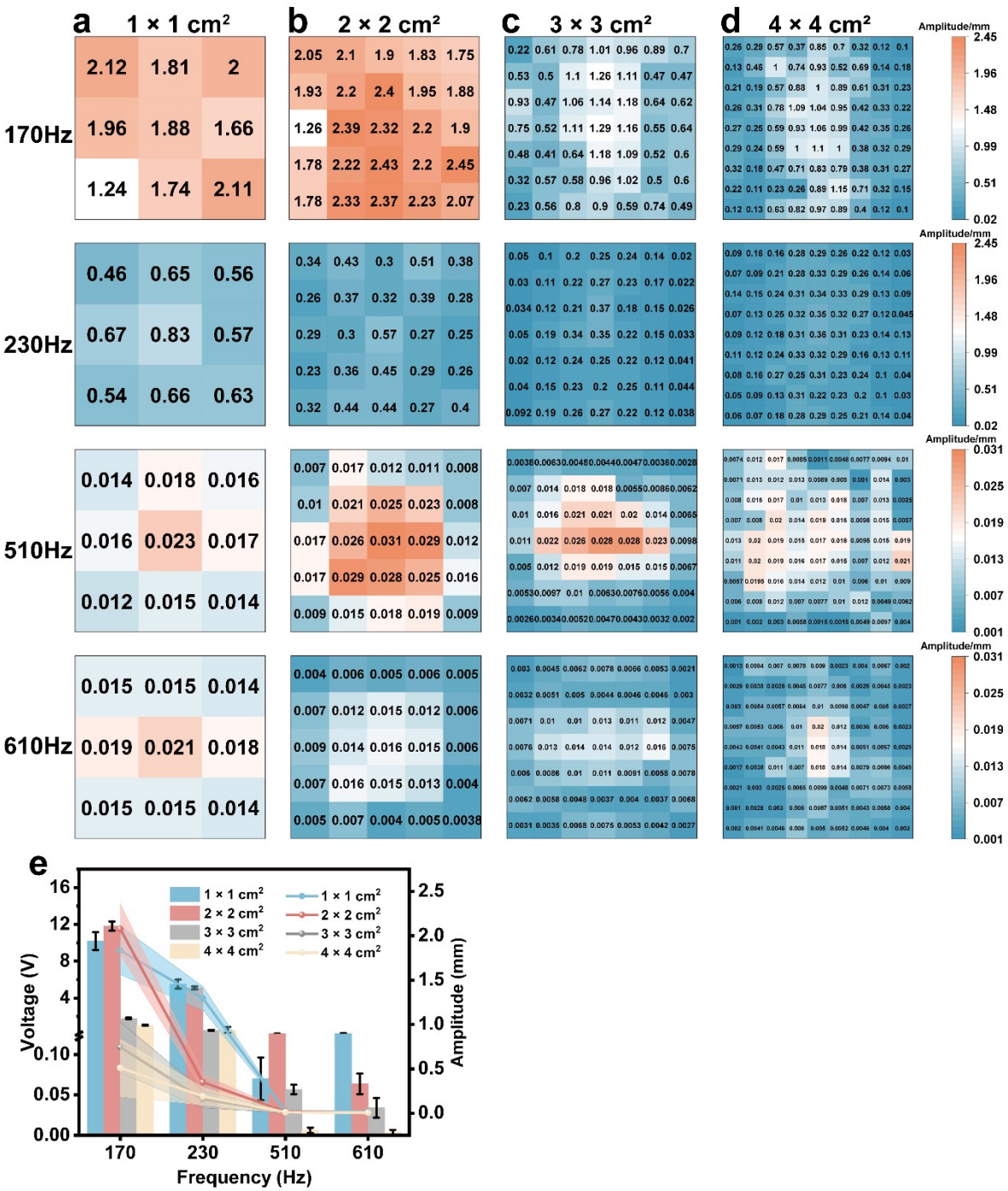

Fig. S6: Vibration testing results of ASF with different sizes. (a) 1 × 1 cm^2, (b) 2 × 2 cm^2, (c) 3 × 3 cm^2, and (d) 4 × 4 cm^2, (e) Comparison chart of vibration conditions and corresponding output voltages for ASFs of four different sizes.

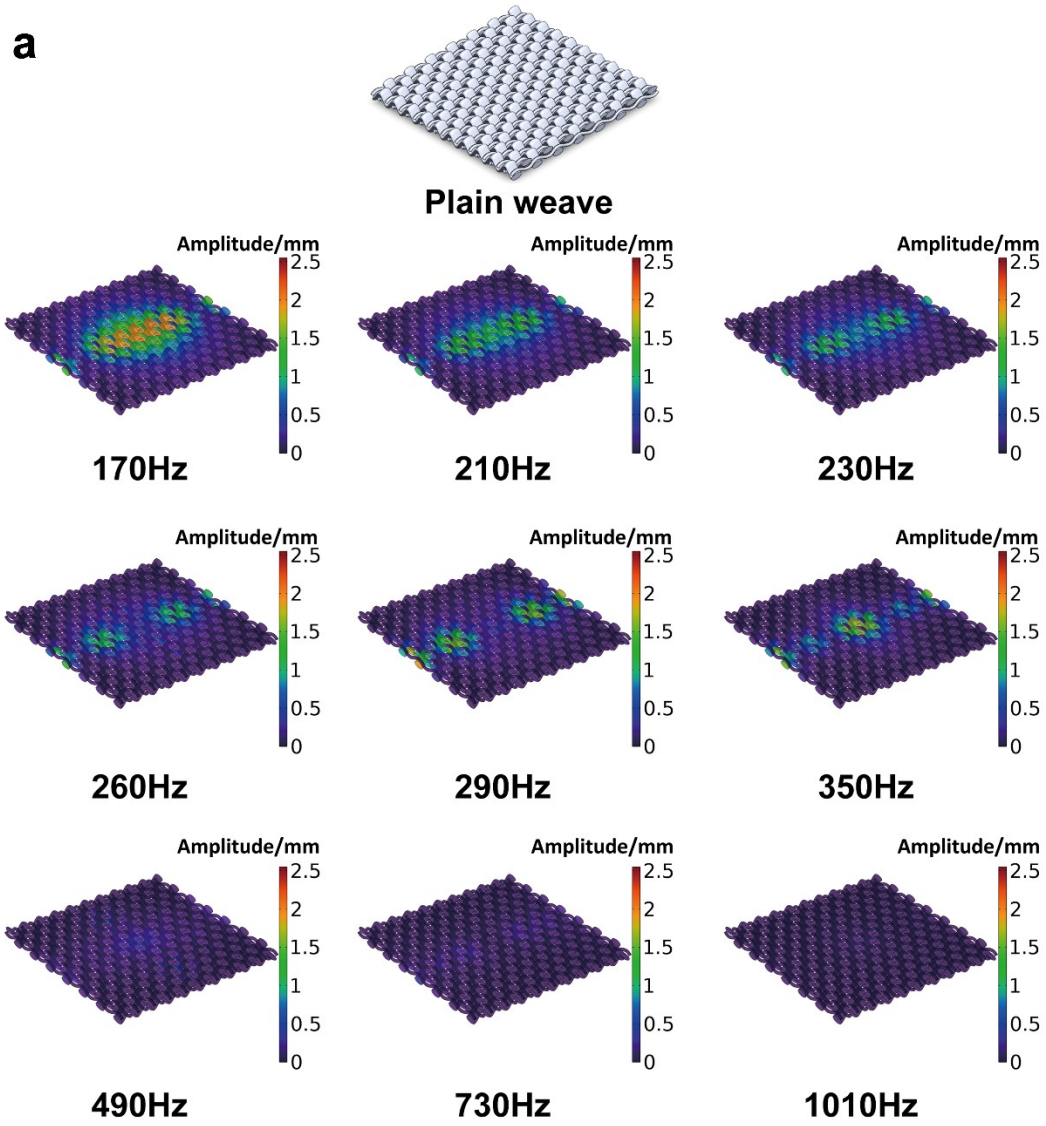
a
Plain weave
Amplitude/mm
2.5
2
1.5
1
0.5
0
170Hz
210Hz
230Hz
260Hz
290Hz
350Hz
490Hz
730Hz
1010Hz

b

1/2 Twill weave

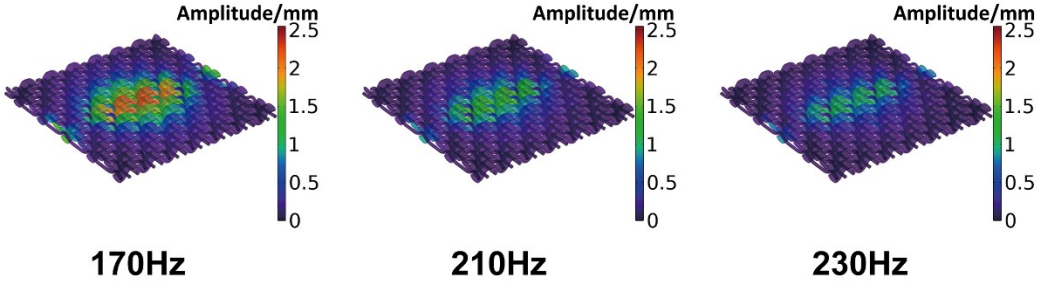

170Hz 210Hz 230Hz

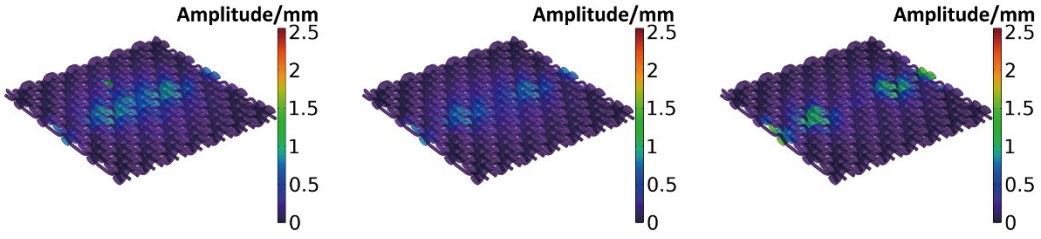

260Hz 290Hz 350Hz

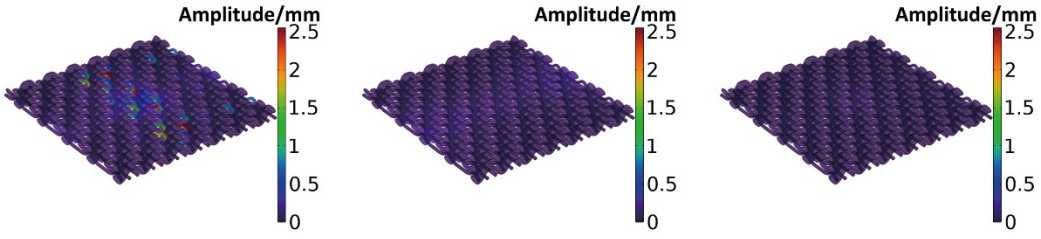

490Hz 730Hz 1010Hz

c

1/3 Twill weave

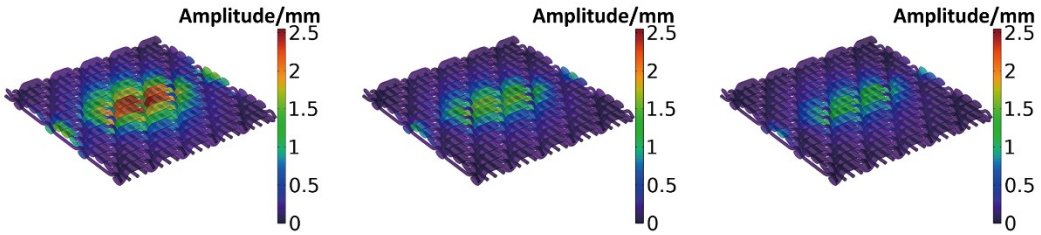

170Hz 210Hz 230Hz

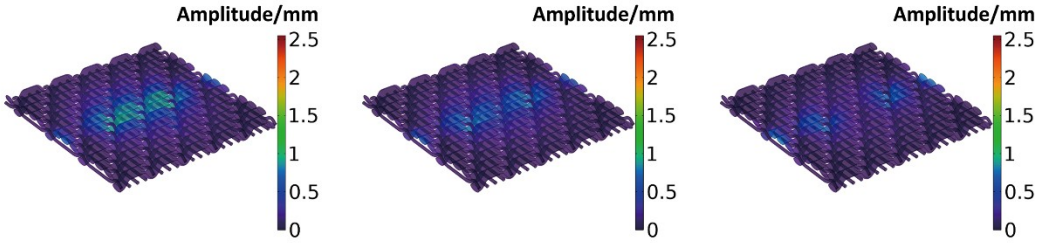

260Hz 290Hz 350Hz

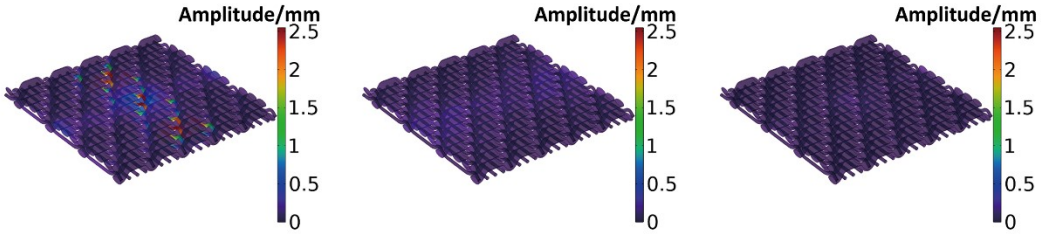

490Hz 730Hz 1010Hz

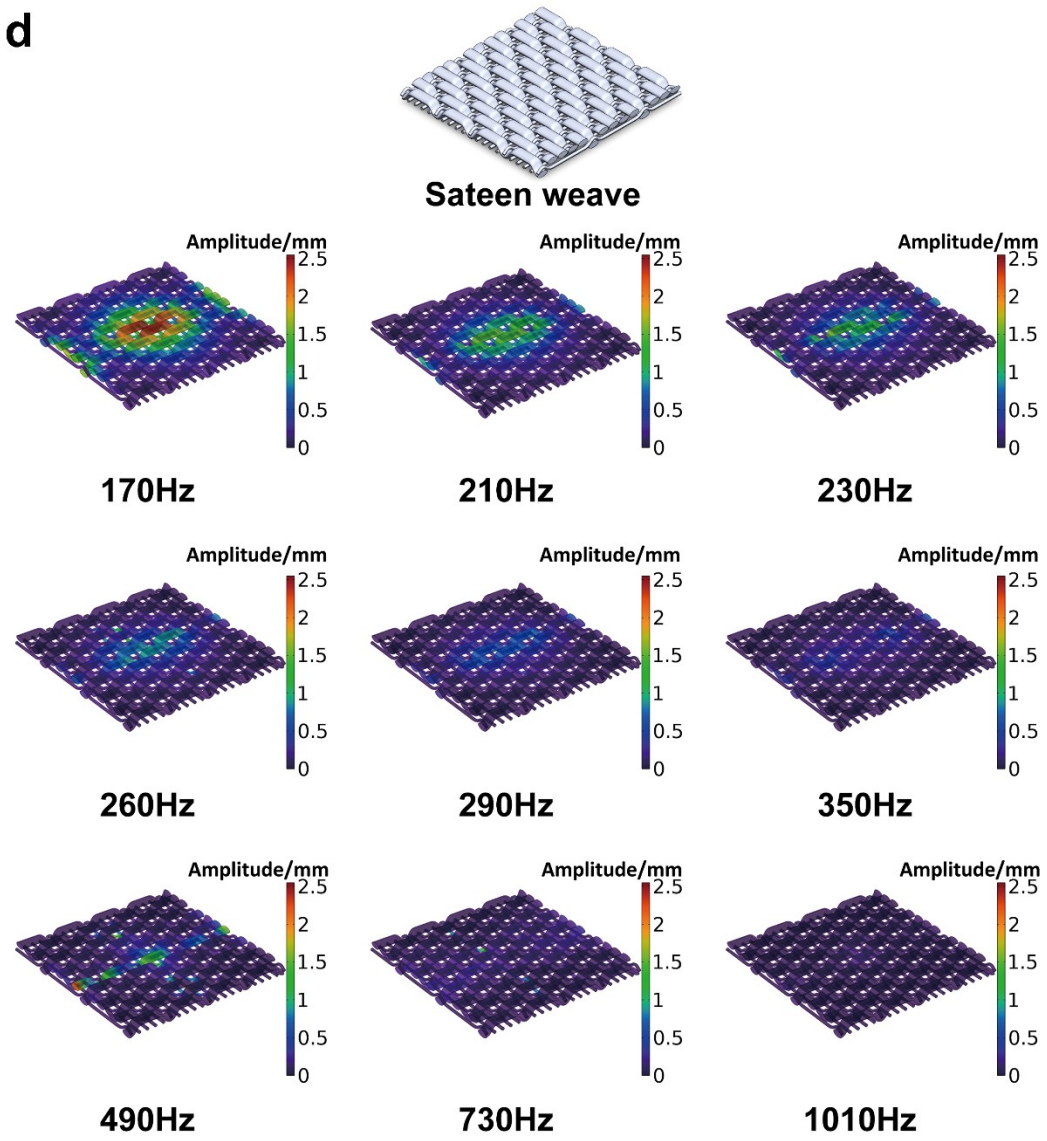

Fig. S7: Simulation test results for different fabric weaves. (a) plain weave, (b) 1/2 twill weave, (c) 1/3 twill weave, and (d) sateen weave.

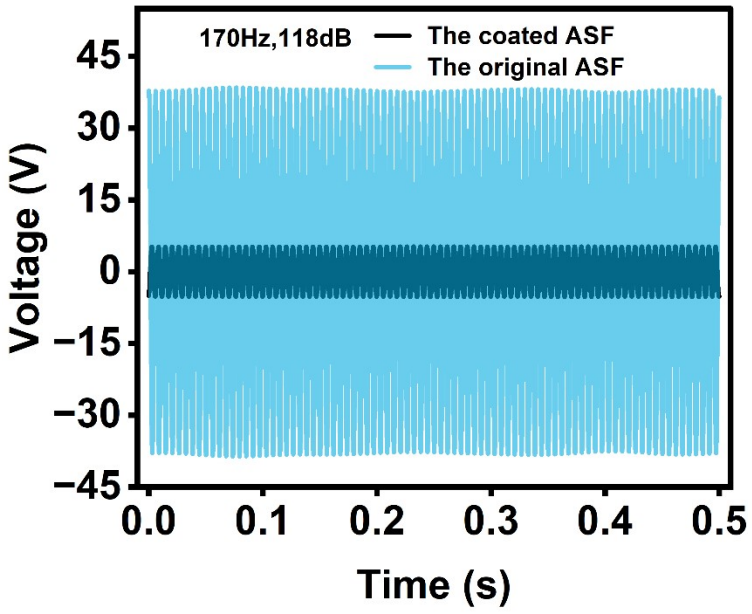

Fig. S8: The output voltage plot of the coated ASF and original ASF.

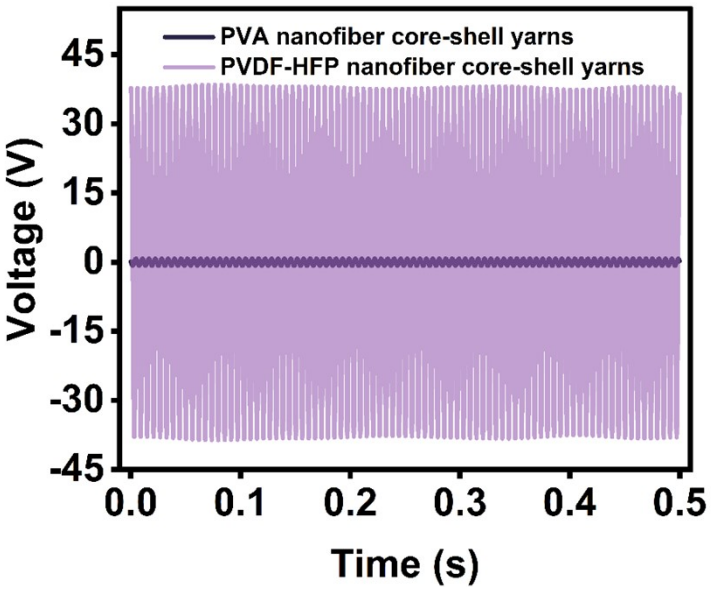

Fig. S9: Electrical output plot measured using PVA nanofiber core-shell yarns and P(VDF-HFP) nanofiber core-shell yarns as weft yarns, respectively.

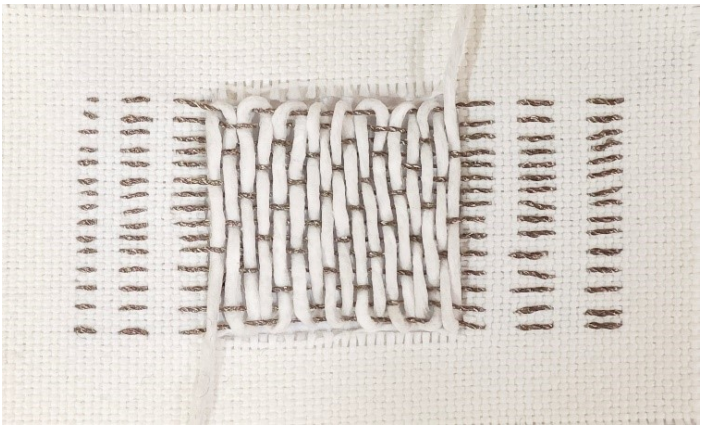

Fig. S10: The digital image of the integration of ASF with conventional textiles

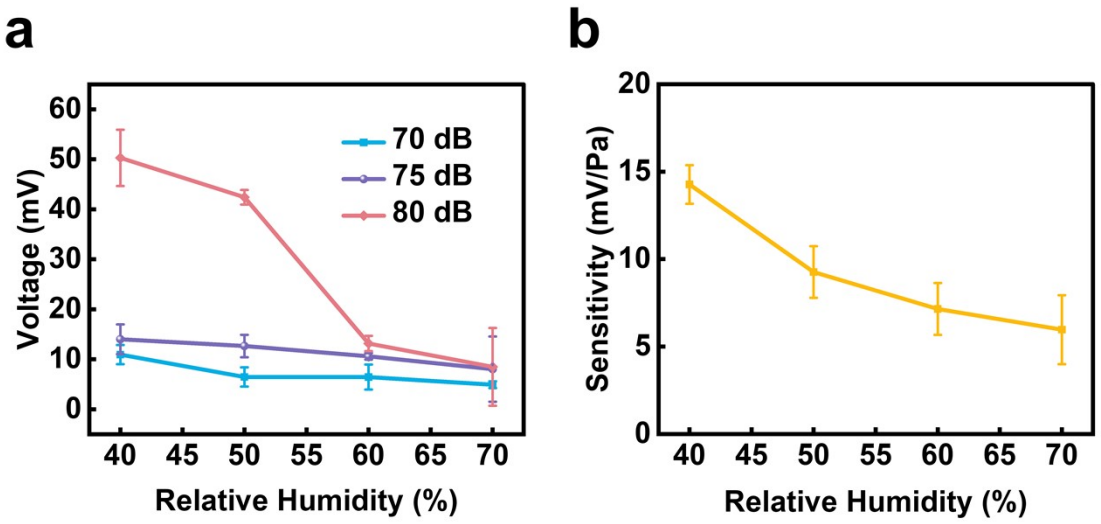

Fig. S11: (a) Output voltage of ASF under different humidity conditions (70-85 dB/170Hz), (b) Sensitivity of ASF under different humidity conditions (94 dB/1000 Hz).

References

1 M.O.G. Nayeem, S. Lee , H. Jin , N. Matsuhisa, H. Jinno, A. Miyamoto , T. Yokota, T. Someya, *Langmuir*, 2020, **117**, 7063-7070.

2 H. Shao, Q.R. Cai, H.B. Jiang, R.U.R. Sagar, S. Mateti, G. Sathikumar, B.Z. Yu, S.M. Huang, Y.L. Chen, *Nano Energy*, 2024, **121**, 109195.

3 F. Mokhtari, K. A. S. Usman, J.Z. Zhang, R. Komljenovic, Ž. Simon, B. Dharmasiri, A. Rezk, P.C. Sherrell, L.C. Henderson, R.J. Varley, J.M. Razal, *ACS Appl. Mater. Interfaces*, 2025, **17**, 3214-3228.

4 K. Roy, S. Jana, Z. Mallick, S.K. Ghosh, B. Dutta, S. Sarkar, C. Sinha, D. Mandal, *Langmuir*, 2021, **37**, 7107-7117.

5 Y. Jiang, Y.F. Zhang, C. Ning, Q.Q. Ji, X. Peng, K. Dong, Z.L. Wang, *Small*, 2022, **18**, 202106960.

6 F. Mokhtari , S. Danti , B. Azimi, F. Hellies, E. Zanoletti, G. Albertin, L. Astolfi, R. J. Varley , J. M. Razal, Energy Environ. Mater., 2025, **8**, e12807.

7 W. Yan, G. Noel, G. Loke, E. Meiklejohn, T. Khudiyev, J. Marion, G.C. Rui, J. Lin, J. Cherston, A. Sahasrabudhe, J. Wilbert, I. Wicaksono, R.W. Hoyt, A. Missakian, L. Zhu, C. Ma, J. Joannopoulos, Y. Fink, *Nature*, 2022, **603**, 616-623.

8 M.L. Zhang, H.Y. Su, C. Zhang, X.Y. Wen, *Measurement*, 2025, **242**, 116044.